Transgenic expression of *Haemonchus contortus* cytochrome P450 *Hco-cyp-13A11* decreases susceptibility to particular but not all macrocyclic lactones in the model organism *Caenorhabditis elegans*

Natalie Jakobs, Esra Yilmaz and Jürgen Krücken *

Institute for Parasitology and Tropical Veterinary Medicine, Freie Universität Berlin, 14163 Berlin, Germany; nataliejakobs@web.de (N.J.); esrayz@msn.com (E.Y.)

* **Correspondence: juergen.kruecken@fu-berlin.de; Tel.: +49 (0) 30 838 62318**

Supplementary Materials: The following are available online at www.mdpi.com/xxx/s1, Figure S1: Vector design of expression plasmid., Figure S2: Comparison of thrashes per minute between the N2 and the transgenic *Hco-cyp-13A11 C. elegans*. Figure S3: Multiple sequence alignment of *Hco-cyp-13A11* amplified coding DNA sequences obtained by assembling exon regions from the genomic sequences., Figure S4: B-factor diagrams of Hco-Cyp-13A11 homology models represented by the B-factor putty program in PyMOL., Figure S5: Molecular docking analysis of Cyp-3A4., Figure S6: Molecular docking analysis of inbred-susceptible isolate Hco-Cyp-13A11., Figure S7: Molecular docking analysis of McMaster Hco-Cyp-13A11., Figure S8: Molecular docking analysis of White River Hco-Cyp-13A11.
Table S1: Primer sequences used for RT-PCR and assembly of plasmid construct., Table S2: Primer sequences used to amplify *Hco-cyp-13A11* exon encoding genomic regions., Table S3: Template alignment and sequence analysis of Hco-Cyp-13A11., Table S4: Parameters for evaluation of the best DOPE score model generated by Modeller., Table S5: Predicted positions of human Cyp-3A4 involved in substrate and heme cofactor binding and corresponding amino acids for Cyp-13A11 in different *Haemonchus contortus* isolates from amino acid sequence alignment and molecular docking of the heme cofactor., Table S6: Amino acids interacting with different macrocyclic lactones from molecular docking analysis.

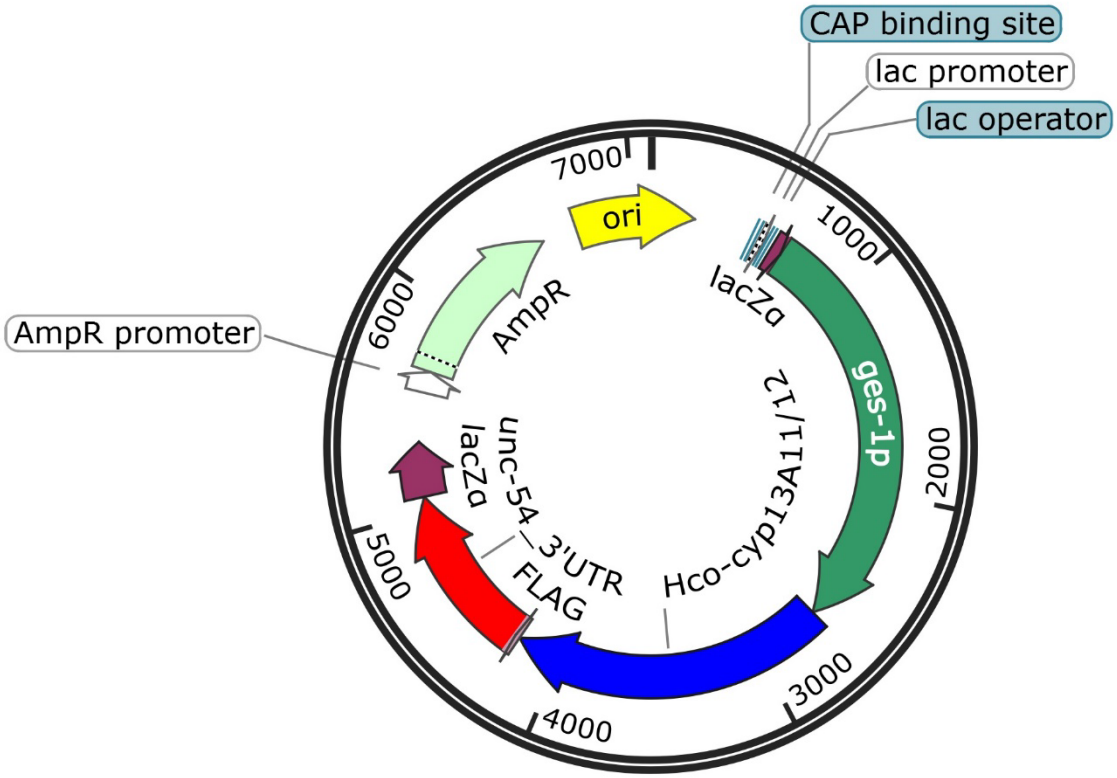

Figure S1: Vector design of expression plasmid. Vector map of plasmid driving extrachromosomal *Hco-cyp-13A11* expression generated with SnapGene (version 5.3). The pUC19 vector backbone contains elements for bacteria-specific replication and selection. *ges-1p*: *C. elegans ges-1* promoter; *Hco-cyp-13A11*: HCON_00141052, BioProject PRJEB506; *unc-54_3'UTR*: *C. elegans unc-54 3'-UTR* (untranslated region); FLAG: Flag-tag GAT TAT AAA GAT GAC GAT GAC AAA or DYKDDDDK (protein sequence).

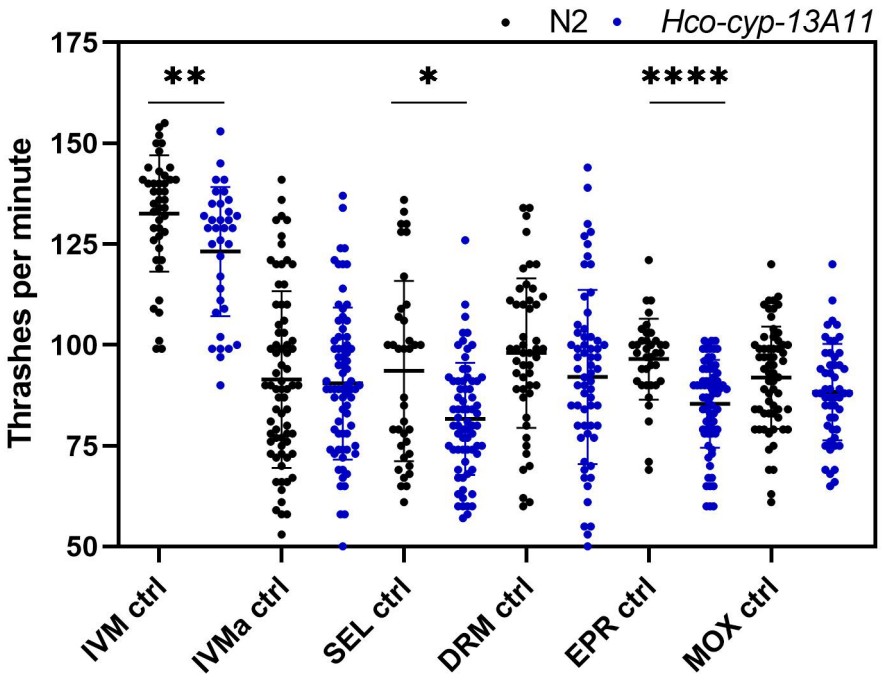

Figure S2: Comparison of thrashes per minute between the N2 and the transgenic *Hco-cyp-13A11 C. elegans*. The Mann Whitney *U* test was used to compare the thrashes per minute from all DMSO N2 controls (**black**) versus all DMSO controls of the transgenic *Hco-cyp-13A11 C. elegans* strain (**blue**) for each corresponding drug test (* $p = 0.0153$, ** $p = 0.0055$, **** $p<0.0001$). *Hco-cyp-13A11* genotype is *gutCyp-13A11Ex1 [Cel-ges-1p::Hco-cyp-13A11::FLAG::Cel-unc-54_3'-UTR; Cel-myo-2p::gfp::Cel-unc-54_3'UTR]*; control strain is N2 Bristol wild-type; ctrl: control; IVM: ivermectin; MOX: moxidectin; EPR: eprinomectin; IVMa: ivermectin aglycone; SEL: selamectin; DRM: doramectin.

Figure S3: Multiple sequence alignment of *Hco-cyp-13A11* amplified coding DNA sequences obtained by assembling exon regions from the genomic sequences. Sequences were derived from different *Haemonchus contortus* isolates with HCON_00141052 (Accession no. LS997566, BioProject PRJEB506) as the reference sequence. Alignment was obtained using Clustal Omega (version 1.2.4) and shading created with BoxShade (version 3.21) with black letters presenting dissimilarities to the consensus sequence.

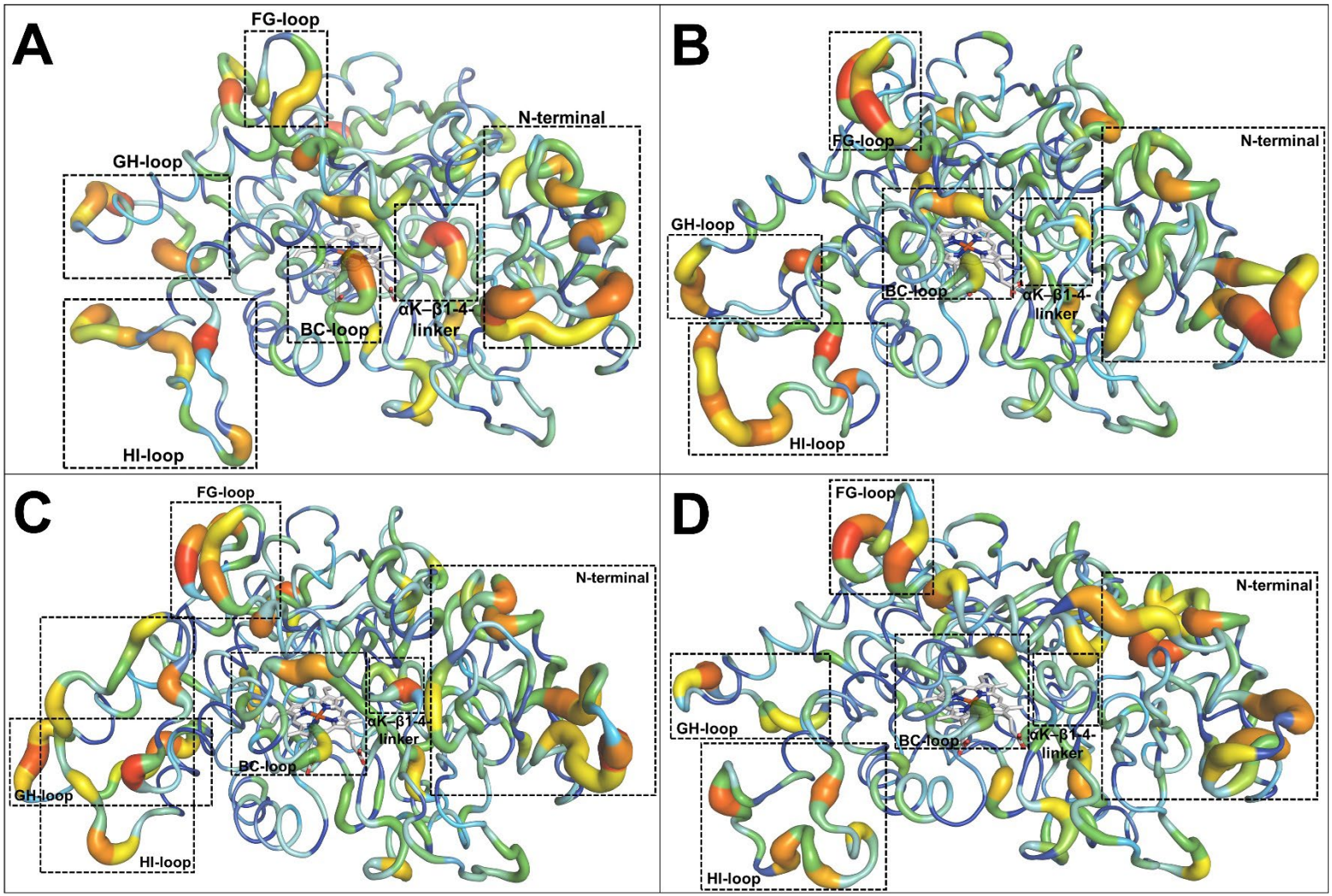

Figure S4: B-factor diagrams of Hco-Cyp-13A11 homology models represented by the B-factor putty program in PyMOL. **A** Inbred-susceptible Edinburgh. **B** McMaster. **C** Berlin-selected Isolate. **D** White River. The B-factor values are illustrated by color ranging from low (blue) to high (red) flexibility with highly flexible loops labeled.

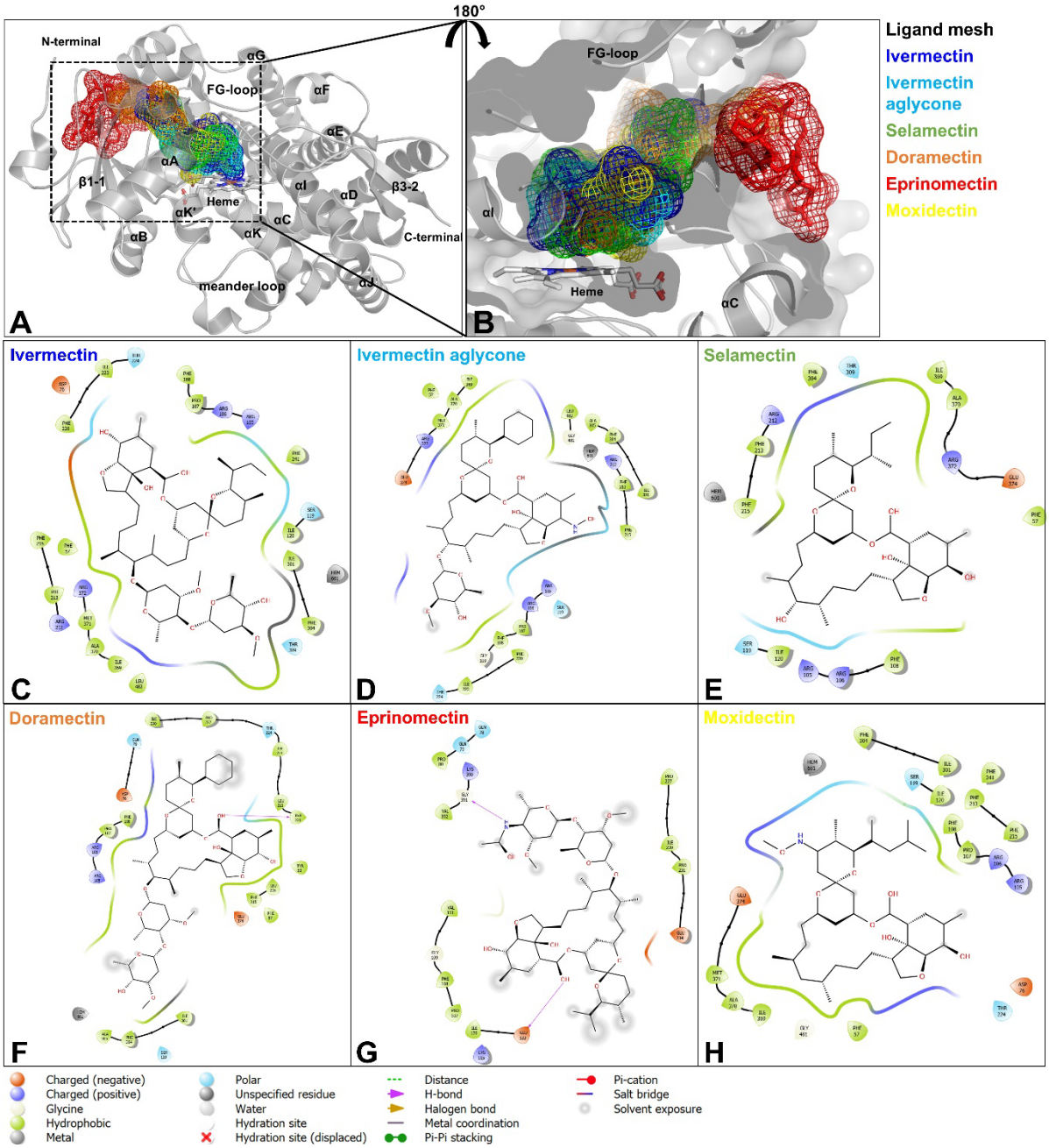

Figure S5: Molecular docking study of Cyp-3A4. **A, B** Overlayed structures of the human Cyp-3A4 (PDB: 6MA7) in complex with IVM (blue), IVMa (cyan), SEL (green), DRM (orange), EPR (red), and MOX (yellow). Ivermectin (**C**), IVMa (**D**), SEL (**E**), and MOX (**H**) docked to the active site cavity. DRM (**F**) and EPR (**G**) docked within a channel towards the active site. The 2D ML ligand-protein interaction diagrams show the closest residues within a 4 Å radius. 2D interaction plots were generated using Maestro Elements (version 4.6.117).

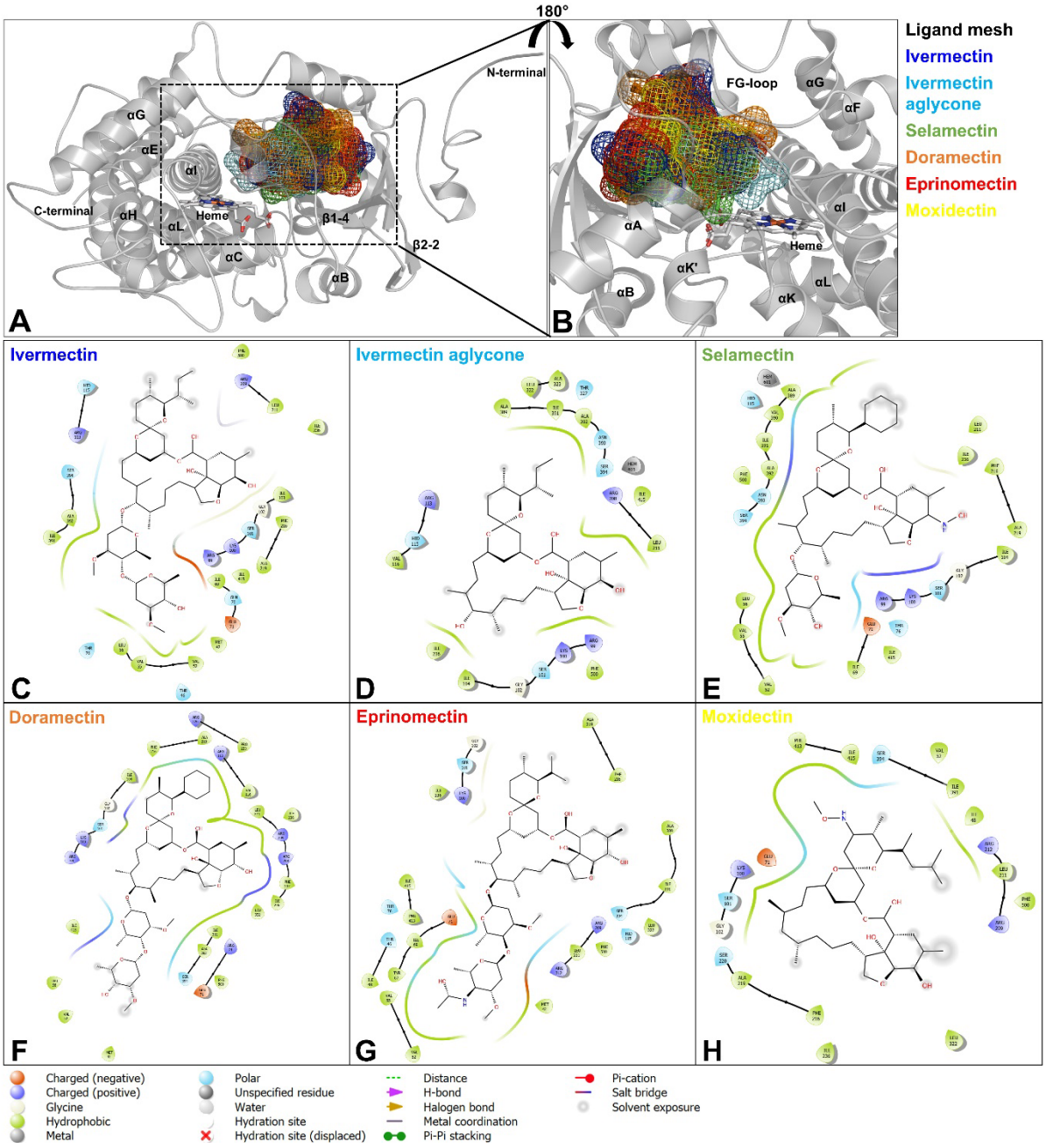

Figure S6: Molecular docking study of inbred-susceptible isolate Hco-Cyp-13A11. **A, B** Overlayed structures of the Hco-Cyp-13A11 Inbred-susceptible Edinburg isolate in complex with IVM (blue), IVMa (cyan), SEL (green), DRM (orange), EPR (red), and MOX (yellow) from different perspectives. IVM (**C**), IVMa (**D**), SEL (**E**), DRM (**F**), EPR (**G**) and MOX (**H**) docked to the active site cavity. The 2D ML ligand-protein interaction diagrams show the closest residues within a 4 Å radius. 2D interaction plots were generated using Maestro Elements (version 4.6.117).

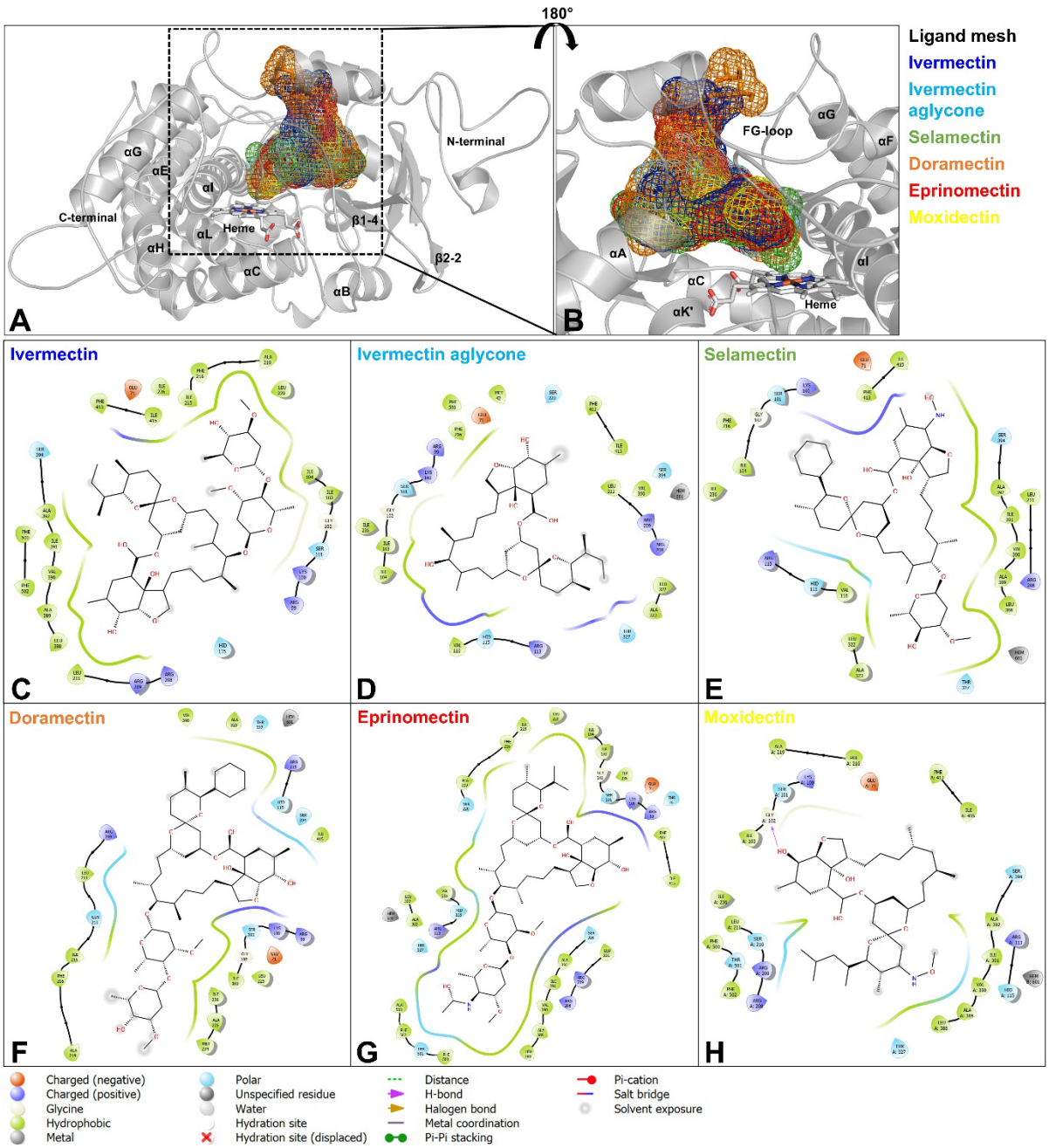

Figure S7: Molecular docking analysis of McMaster Hco-Cyp-13A11. **A, B** Overlayed structures of the Hco-Cyp-13A11 McMaster isolate in complex with IVM (blue), IVMa (cyan), SEL (green), DRM (orange), EPR (red), and MOX (yellow) from different perspectives. IVM (**C**), IVMa (**D**), SEL (**E**), DRM (**F**), EPR (**G**) and MOX (**H**) docked to the active site cavity. The 2D ML ligand-protein interaction diagrams show the closest residues within a 4 Å radius. 2D interaction plots were generated using Maestro Elements (version 4.6.117).

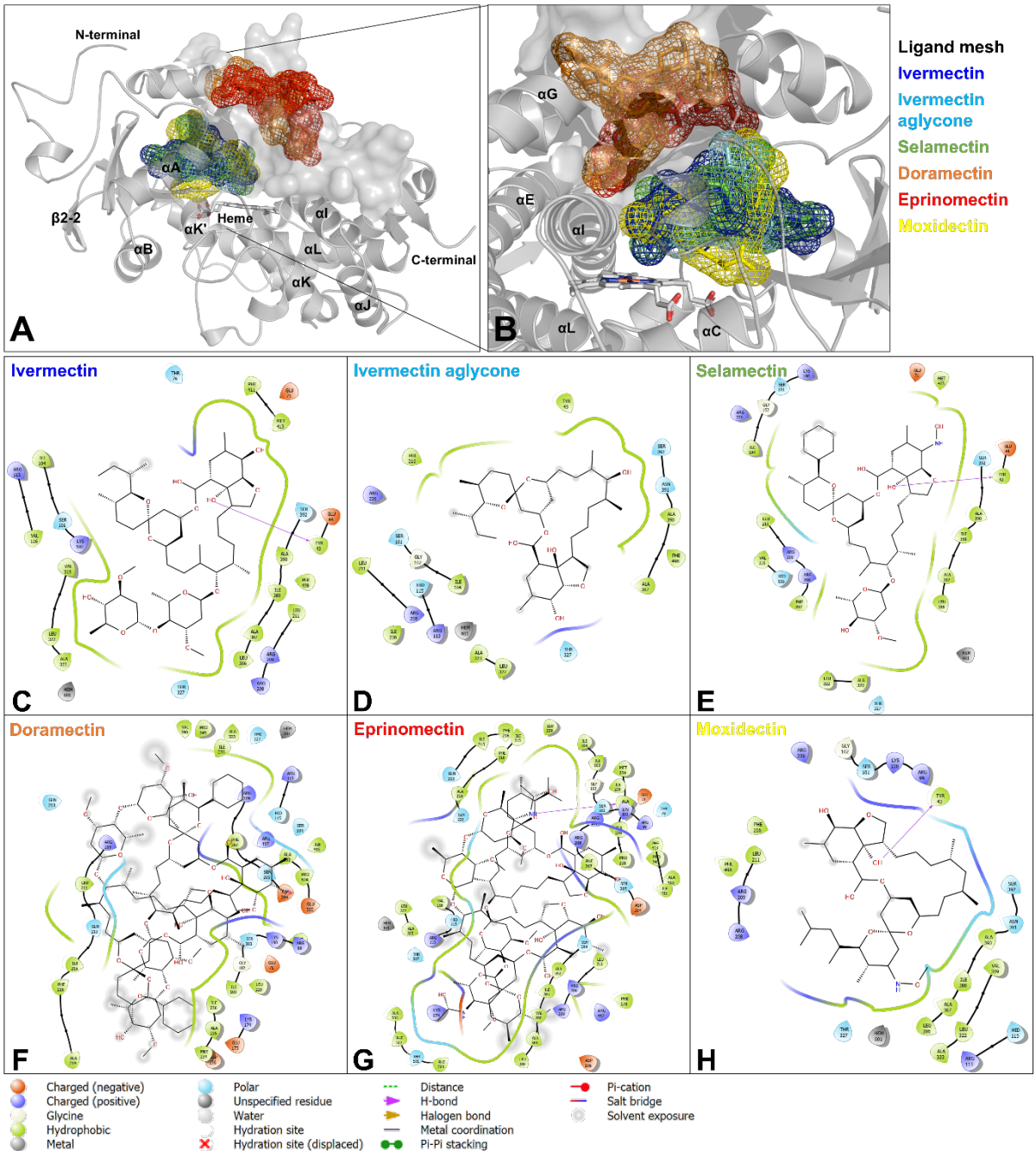

Figure S8: Molecular docking analysis of White River Hco-Cyp-13A11. **A, B** Overlayed structures of the Hco-Cyp-13A11 Berlin-selected isolate in complex with IVM (blue), IVMa (cyan), SEL (green), DRM (orange), EPR (red), and MOX (yellow) from different perspectives IVM (**C**), IVMa (**D**), SEL (**E**), and MOX (**H**) docked to the active site cavity. DRM (**F**) and EPR (**G**) showed the lowest binding energy docked at the outer surface of the FG-loop. The 2D ML ligand-protein interaction diagrams show the closest residues within a 4 Å radius. 2D interaction plots were generated using Maestro Elements (version 4.6.117).

Table S1: Primer sequences used for RT-PCR and assembly of plasmid construct. Assembly primers were designed using NEBuilder®Assembly Tool (version 2.3.1).

Purpose	Primer	Direction	Primer sequence (5'→3')	Size [bp]	Elongation time [s]	Annealing temperature [°C]
Assembly	pUC19_ges-1	fwd[a]	cgacggccagtgaattcgagctcggtacccAAACTCCGAACTATGATGAC	2000	30	55.6
	Hco-cyp-13A11_ges-1	rev[b]	gataagcaaaagcatCTGAATTCAAAGATAAGATATGTAATAG			
Assembly and RT-PCR	ges-1_Hco-cyp-13A11	fwd	tatctttgaattcagATGCTTTTGCTTATCATCG	1552	30	57.8
	unc54UTR_Hco-cyp-13A11	rev	catcgtcatctttataatcTAAGTGTTCTCTTCGTTGTAGC			
Assembly	Hco-cyp-13A11_unc54UTR	fwd	cgaagagaacacttagattataaagatgacgatgacaaatagGTCCAATTACTCTTCAACATC	848	30	55.1
	pUC19_unc54UTR	rev	atgcctgcaggtcgactctagaggatccccCCGGAAAACACAATAATG			

[a] fwd: forward.

[b] rev: reverse.

Table S2: Primer sequences used to amplify *Hco-cyp-13A11* (HCON_00141052, Accession no. LS997566, BioProject PRJEB506) exon encoding genomic regions to compare the sequences for different *Haemonchus contortus* isolates.

***Haemonchus contortus* isolate**	**(Overspanning) Exon region**	**Primer**	**Primer sequence (5'→3')**	**Amplicon length (bp)**	**Elongation time [s]**	**Annealing temperature [°C]**
White River	1, 2	fwd[a]	TGGTCACCTTTCGTCATCGG	1077	40	69.3
		rev[b]	GAATTCCTCGCCGCTTCCAG			
	2, 3, 4	fwd	ACTTACAGCTATTACTACTGGCAA	597	30	60.5
		rev	TGTGAGTCAACGCACCTTCT			
	5, 6, 7	fwd	CTCTTTAGATCCGCCCAACTGT	501	30	62.4
		rev	TTTTAATCAACCAAACCTCAGAGG			
	8, 9	fwd	CGTTCTTGCCGTTCGATTGT	429	30	64.4
		rev	CGAGCTTGAACCGTTTTCTCG			
	10, 11, 12	fwd	GCCATCATTACAGGTTACAAAGCA	617	40	61.5
		rev	CCTTTCAGGTCTAAATTCCTCTGC			
	13	fwd	AGATGGACTGAGTTGACGGC	162	15	63.9
		rev	CACCTCGGTATCATTTGTTGCA			
	14	fwd	AGTCCTCGAAGTCTCGGTCA	227	15	62.4
		rev	CTCACGAGGAACAACCACCA			
Berlin-Selected Isolate	1, 2	fwd	TGGTCACCTTTCGTCATCGG	1077	40	68.2
		rev	GAATTCCTCGCCGCTTCCAG			
	2, 3, 4	fwd	AGTCAATAAAGTAGGTGGAGACGT	694	30	63.0
		rev	GCTTCGGTACCCCTGAAACC			
	5, 6, 7	fwd	CTCTTTAGATCCGCCCAACTGT	501	30	60.9
		rev	TTTTAATCAACCAAACCTCAGAGG			
	8, 9	fwd	CGTTCTTGCCGTTCGATTGT	429	30	64.4
		rev	CGAGCTTGAACCGTTTTCTCG			
	10, 11, 12	fwd	TGCTTCAGAAATGGCCATCA	603	40	60.5
		rev	GCACGATTCCTACCTCAGCA			
	13	fwd	AGATGGACTGAGTTGACGGC	162	15	62.4
		rev	CACCTCGGTATCATTTGTTGCA			
	14	fwd	AGTCCTCGAAGTCTCGGTCA	227	15	61.9
		rev	CTCACGAGGAACAACCACCA			
Inbred-Susceptible Edinburgh	1, 2	fwd	TGGTCACCTTTCGTCATCGG	1077	40	69.3
		rev	GAATTCCTCGCCGCTTCCAG			
	2, 3, 4	fwd	AGTCAATAAAGTAGGTGGAGACGT	694	30	63.0
		rev	GCTTCGGTACCCCTGAAACC			
	5, 6, 7	fwd	CTCTTTAGATCCGCCCAACTGT	501	30	60.9
		rev	TTTTAATCAACCAAACCTCAGAGG			
	8, 9	fwd	CGTTCTTGCCGTTCGATTGT	429	30	64.4
		rev	CGAGCTTGAACCGTTTTCTCG			
	10, 11, 12	fwd	TGCTTCAGAAATGGCCATCA	603	40	60.5
		rev	GCACGATTCCTACCTCAGCA			
	13	fwd	AGATGGACTGAGTTGACGGC	162	15	62.4
		rev	CACCTCGGTATCATTTGTTGCA			
	14	fwd	AGTCCTCGAAGTCTCGGTCA	122	15	61.9
		rev	CTCACGAGGAACAACCACCA			
McMaster	1	fwd	CTCTAGCGATACGACGGTG	115	40	61.0
		rev	AGTTCAAGGTACCTTATGAAAGCT			
	2, 3, 4	fwd	GGTTTGAAAGACTTACTTACAGCT ATT	611	30	63.1
		rev	TGTGAGTCAACGCACCTTCT			
	5, 6, 7	fwd	CTCTTTAGATCCGCCCAACTGT	501	30	60.9
		rev	TTTTAATCAACCAAACCTCAGAGG			
	8, 9	fwd	CGTTCTTGCCGTTCGATTGT	429	30	63.3
		rev	CGAGCTTGAACCGTTTTCTCG			
	10, 11, 12	fwd	TGCTTCAGAAATGGCCATCA	617	40	61.4
		rev	GCACGATTCCTACCTCAGCA			
	13	fwd	AGATGGACTGAGTTGACGGC	162	15	63.3
		rev	CACCTCGGTATCATTTGTTGCA			
	14	fwd	CCTCGAAGTCTCGGTCACAA	122	15	63.4
		rev	TGCTGTTCATAAGTGTTCTCTTCG			

Table S3: Template alignment and sequence analysis of Hco-Cyp-13A11 for the isolates Inbred-Susceptible Edinburgh (ISE), McMaster (McM), White River (WR), and Berlin-Selected Isolate (BSI) used for single alignment modeling.

Protein	Organism	PDB ID	Resolution [Å]	Inhibitor[c]	Sequence identity (%)				E-value				Chain length
					ISE	McM	WR	BSI	ISE	McM	WR	BSI	
Cyp-3A4	*Homo sapiens*	6MA7[a]	2.09	Fluconazole	28.71%	28.92%	28.97%	28.92%	5e-58	5e-59	8e-60	1e-58	487
Cyp-3A4	*Homo sapiens*	4D6Z[a]	1.93	Tert-butyl {6-oxo-6-[(pyridin-3-ylmethyl)amino]hexyl} carbamate	29.32%	29.52%	29.58%	29.32%	4e-57	4e-58	6e-59	8e-58	487
Cyp-3A4	*Homo sapiens*	5A1R[b]	2.45	Progesterone	28.39%	28.60%	31.29%	31.22%	-	-	-	-	478

[a] The modeling templates were selected based on protein BLAST search (NCBI server).

[b] The modeling template was selected based on the SwissModel Template Search web tool (https://swissmodel.expasy.org/interactive). E-values are not given by the SwissModel Template Search web tool.

[c] Small molecule inhibitors bound the proteins when crystallized.

Table S4: Parameters for evaluating the best DOPE score model generated by Modeller (version 10.1) based on single alignment modeling and individual loop refinement.

	Inbred-susceptible Edinburgh[e]	**McMaster**	**White River**	**Berlin-selected Isolate**
Modeller				
Dope-Score	-58285	−59162	−58290	−57995
Prosa-web[a]				
Z-score	-7.66	−8.06	−7.64	−7.57
Errat[b]				
Overall quality factor	61.46	61.78	48.12	53.84
QMEAN3[c]				
QMEAN score	0.60 (Z-score: -5.24)	0.62 (Z-score: −4.72)	0.61 (Z-score: −4.79)	0.62 (Z-score: −4.49)
ProCheck Ramachandran plot[d]				
Residues in most favored regions	409 (87.0%)	422 (89.4%)	415 (88.3%)	419 (88.8%)
Residues in additional allowed regions	53 (11.3%)	39 (8.3%)	44 (9.4%)	45 (9.5%)
Residues in generously allowed regions	7 (1.5%)	10 (2.1%)	8 (1.7%)	5 (1.1%◎)
Residues in disallowed regions	1 (0.2%)	1 (0.2%)	3 (0.6%)	3 (0.6%)
Number of non-glycine and non-proline residues	470 (100.0%)	472 (100.0%)	470 (100.0%)	472 (100.0%)
Number of end-residues	2	2	2	2
Number of glycine residues	28	26	26	26
Number of proline residues	17	17	17	17

[a] Predicted by https://prosa.services.came.sbg.ac.at/prosa.php.

[b] Predicted by https://saves.mbi.ucla.edu/.

[c] Predicted by https://swissmodel.expasy.org/qmean/.

[d] Predicted by https://saves.mbi.ucla.edu/.

[e] The inbred-susceptible Edinburgh sequence was obtained by exon sequencing.

Table S5: Predicted positions of human Cyp-3A4 involved in substrate and heme cofactor binding and corresponding amino acids for Cyp-13A11 in different *Haemonchus contortus* isolates from amino acid sequence alignment and molecular docking of the heme cofactor.

Function	Cyp-3A4[a]	Hco-Cyp-13A11			
		ISE[b]	McM[c]	BSI[d]	WR[e]
Control of substrate specificity and regioselectivity (Sirim et al., 2010)	Ser119	Phe117	Phe117	Phe117	Phe117
Roof of the active site (Yano et al., 2004a)	Leu210	Ile206	Ile206	Ile206	Ile206
	Phe213	Arg209	Arg209	Arg209	Arg209
	Phe215	Leu211	Leu211	Leu211	Leu211
Allostery and stereoselectivity	Leu210	Ille206	Ille206	Ille206	Ille206
	Leu211	Phe207	Phe207	Phe207	Phe207
	Asp214	Ser210	Ser210	Ser210	Ser210
Position a water molecule for proton transfer (Yano et al., 2004a)	Glu308	Glu326	Glu326	Glu326	Glu326
	Thr309	Asp327	Asp327	Asp327	Asp327
Active site residues (Yano et al., 2004a)	Ser119	Phe117	Phe117	Phe117	Phe117
	Ile301	Phe319	Phe319	Phe319	Phe319
	Phe304	Phe322	Phe322	Phe322	Phe322
	Ala305	Leu323	Leu323	Leu323	Leu323
	Ile369	Leu388	Leu388	Leu388	Leu386
	Ala370	Ala389	Ala389	Ala389	Ala387
	Glu374	Ser394	Ser394	Ser394	Ser392
Coordination of Heme propionates (Williams, 2004) and polar interaction sites[f,g,h]	Arg105	*Arg99*	*Arg99*	*Arg99*	*Arg99*
	Ile118	*His115*	**Val114**	**Val114**	*His115*
	Trp126	Trp124	Trp124	Trp124	Trp124
	Arg130	**Arg128**	Arg128	Arg128	Arg128
	Arg375	*Asn393*	*Asn393*	*Asn393*	**Arg391**
	Ser437	Arg395	Arg395	Arg395	Arg393
	Arg440	**Phe454**	**Phe454**	**Phe454**	
		Arg459	Arg459	Arg459	Arg457
Heme-binding (Yano et al., 2004a)	Cys442	Cys461	Cys461	Cys461	Cys459

[a] Predicted position in 1TQN crystal structure (Yano et al., 2004b).

[b] Own Inbred-susceptible Edinburgh *H. contortus* sequence.

[c] McMaster isolate.

[d] Berlin-selected isolate.

[e] White River Isolate.

[f] Non-covalent polar interaction sites predicted by PyMOL in bold.

[g] Hydrogen Bonds computed by PLIP (Adasme et al., 2021) are underlined.

[h] Polar interaction sites predicted by PyMOL and PLIP in cursive.

Table S6: Residues and their corresponding regions within the protein forming hydrogen bonds with the substrates. Only interacting residues for ligand conformations with the lowest docking energy are listed for the human Cyp-3A4 and homology models of Hco-Cyp-13A11. The prediction was performed with the PLIP web tool (Adasme et al., 2021).

			Hco-Cyp-13A11				
Drug	**Region**	**Cyp-3A4 (PDB: 6MA7)**	**Region**	**Inbred-susceptible Edinburgh**	**McMaster**	**White River**	**Berlin-selected isolate**
Ivermectin		Asp76 Arg106 Thr224				Tyr43 Thr76	
			BC-loop	Ile103	Gly102	Arg113	Lys100 Arg113
			FG-loop			Arg209	
			αK-β1-4-linker	Ser394	Leu388 Ser394 Phe500	Ser392	
Ivermectin aglycone		Arg105	BC-loop	Lys100	His115		Lys100
			αK-β1-4-linker	Ser394	Ser394	Ala390	Ser394
Selamectin	BC-loop	Ser119				Tyr43 Glu44	
			BC-loop	Gly102	His115	His115	Lys100 Gly102
			FG-loop			Arg209	
			αK-β1-4-linker		Ser394	Ser392	
Doramectin	BC-loop	Ser119 Phe220 Thr224	BC-loop	Arg113	Lys100 Ile103		
			FG-loop	Arg209		Arg209	Arg209 Gln213
			αK-β1-4-linker	Ser394	Ser394		
			β4-1			Arg495	Arg497
Eprinomectin		Gln79		Thr46			
		Glu122	BC-loop		Gly102		
	β2-2	Gly391	β3-1			Phe170	
			FG-loop		Arg208 Arg209		Arg208 Ala235
			αI			Thr330	
			αK-β1-4-linker	Ala389 Ser394	Ser394		
			β4-1				Arg497
			β4-2		Phe502	Val505	
Moxidectin		Arg105 Arg106 Thr224				Tyr43	Asp47
			BC-loop		Gly102 Arg113	Ser101 Arg113	Lys100
			FG-loop			Arg226	Arg209
			αK-β1-4-linker	Ser394			